# Current Monitoring in a Microchannel with Repeated Constrictions for Accurate Detection of Sample Location in Isotachophoresis

Merav Karsenty, Tally Rosenfeld, Khaled Gommed, and Moran Bercovici*

Faculty of Mechanical Engineering, Technion—Israel Institute of Technology, Haifa 32000, Israel

Ⓢ Supporting Information

ABSTRACT: We present a new method for accurate detection of sample location in peak mode isotachophoresis (ITP). The technique is based on the design of a microchannel with multiple constrictions and on detecting the passage of the ITP interface through these constrictions. We achieve this by monitoring the electric current across the channel, which exhibits sharp decreases as the ITP interface moves more rapidly through the higher current density constrictions. We show that cross-correlation between the electric current signal and a predefined step function is an effective method for detecting changes in the slope of the electric current curve in real-time and is robust to changes in the composition of the buffers. We demonstrate the use of the technique to deliver sample to a designated location in the channel with an accuracy as low as 50 μm. Importantly, the method does not require the use of any optics and thus can be used to monitor the location of unlabeled species for application in a variety of ITP assays.
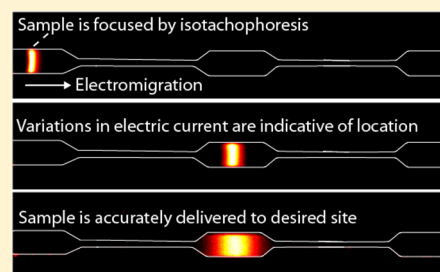
Isotachophoresis (ITP) is an electrophoretic technique allowing focusing and separation of sample molecules based on their effective electrophoretic mobility. ITP uses a discontinuous buffer system consisting of a leading electrolyte (LE) having a high electrophoretic mobility leading ion and a terminating electrolyte (TE) having a low electrophoretic mobility trailing ion. In peak mode ITP, sample ions are focused at a sharp electric field gradient formed at the interface between the two buffers.[1] The ability of ITP to significantly focus trace analytes, from volumes of the order of microliters into well-confined picoliter volumes, established it as an important method in separation science with applications ranging from medical diagnostics to environmental monitoring.[2]

In recent years, the ability to leverage the high concentrations obtained in ITP toward accelerating the reaction kinetics of cofocused species has been studied in detail.[3−8] Acceleration of reactions is particularly important in detection of biomolecules, such as nucleic acids and proteins, where hybridization or binding rates often pose a bottleneck in assay sensitivity. In the past year, at least three groups have further expanded this direction and began exploring the use of ITP for acceleration of surface-based reactions; our group demonstrated the use of ITP for accelerating the hybridization between focused DNA sequences and immobilized DNA probes, leading to 2 orders of magnitude improvement in limit-of-detection (LoD) compared to a standard flow assay.[9] Han et al. have, in parallel, studied a similar system and further expanded it to multiple reaction sites in a DNA microarray format;[10] Khnouf et al. provided a proof of concept where ITP was used for improving the sensitivity of protein detection in a surface immunoassay.[11] These advancements, together with its robustness and ease of implementation in microfluidic devices, position ITP as a promising technology for lab-on-chip applications and, in particular, rapid and sensitive point-of-care diagnostics.

These assays, while presenting a significant improvement in the LoD of surface reactions assays, are still limited by a short reaction time (of the order of 1 s) corresponding to the time it takes the focused sample to traverse the functionalized surface. Further advancement in ITP-based surface reactions relies on the ability to accurately determine the location of the (typically unlabeled) focused sample and deliver it to a designated reaction site. While this could, in principle, be achieved by visual means if the sample is labeled (i.e., human inspection or image processing), there is no existing solution for accurately monitoring the location of an unlabeled sample. Furthermore, aiming to utilize this technology for simple and low-cost point-of-care diagnostics, automating the process and eliminating the need for manual controls are of key importance.

Reading of the electric current during ITP has been long demonstrated as a useful tool for monitoring the velocity and progress of electrophoresis processes. Most notably, Huang et al. demonstrated the use of current monitoring for measuring the electroosmotic flow in channels.[12] Specifically for ITP, Reinhoud et al. developed an analytical model relating the current measurement to the location of the ITP front in a straight channel. They then used the model to design an automated feedback system for counterflow, in order to hold the focusing region stationary.[13] More recently, Harrison et al. developed a similar model relating the electric current to the location of the front for constant applied voltage and have validated it in counterflow ITP performed in a large
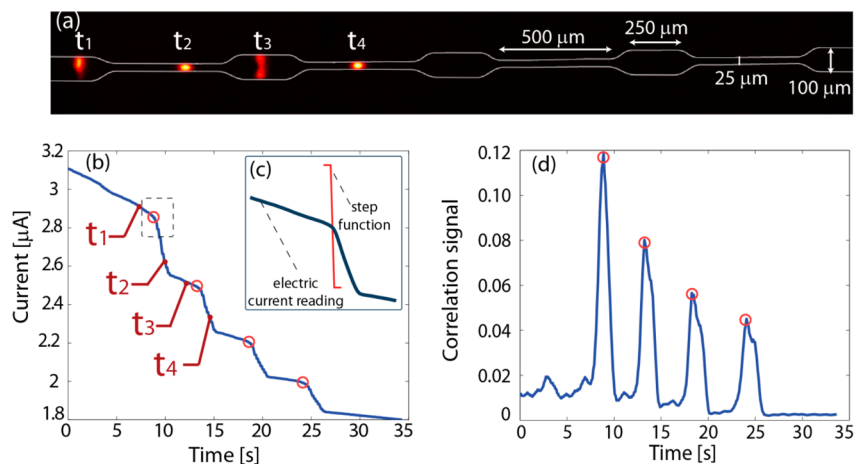
Figure 1. Experimental results demonstrating the use of channel constrictions for accurate determination of ITP plug location. (a) Overlay of four raw fluorescence images showing the location of the sample at different times during electromigration. (b) Corresponding electric current measurement vs time. Electric current monotonically decreases as the low mobility TE displaces the high mobility LE. When the ITP interface enters the constriction, a rapid and significant drop in current occurs. (c) We detect the transitions in real time by cross-correlation of the signal with a predefined step function. Maximum correlation signal is expected when the step function overlaps with the step in the current signal. Red circles indicate the points in time in which the algorithm detects the transition (i.e., local maxima in the cross-correlation). (d) Correlation signal resulting from applying the algorithm to the electric current signal. The method is robust to noise, and peak values (red ○) indicate entrance to the constriction regions. Peaks are recognized by the computer in real-time and the ITP plug can be stopped at a designated location.
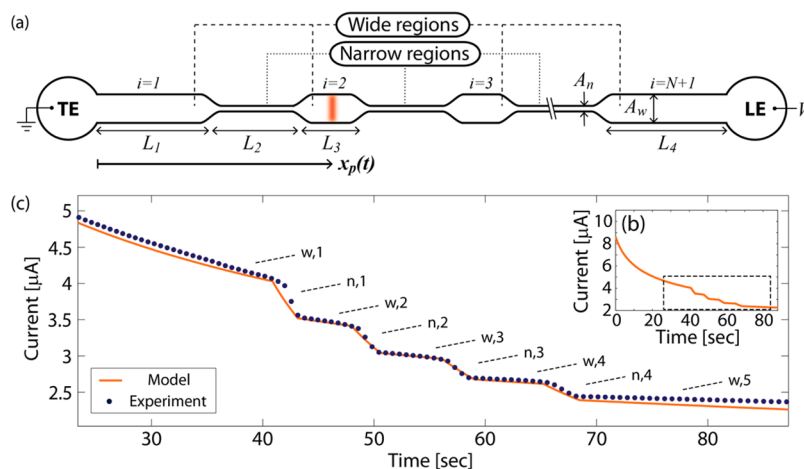

Figure 2. Schematic illustration of our channel, consisting of N constrictions, and demonstration of experimental validation of the model in a typical microchannel, consisting of four constrictions. (a) Four characteristic lengths are denoted by L_1, L_2, L_3, and L_4. The wide and narrow cross-section areas are denoted by A_w and A_n, respectively. Each wide region is indexed by i, ranged between 1 to $N + 1$. The axial position of the ITP interface along the channel is defined by $x_p(t)$. (b) Model results showing a time trace of the electric current for a geometry consisting of $N = 4$ constrictions. We analytically solved eq 7 for $x_p(t)$ and substitute it into eq 1 to obtain the current at any point in time. Four "steps" in the current are registered, corresponding to times at which the ITP interface passes through the constrictions. (c) Comparison of model predictions (solid orange line) with experimental results (black dots) for the constrictions region. Results are in good agreement in both step magnitude and length (duration). The times at which the ITP interface spends in each of the wide and narrow regions are indicated by w,i and n,i, respectively. The model parameters are LE is 100 mM HCl and 200 mM bistris; TE is 10 mM tricine and 20 mM bistris. The applied voltage is 400 V; $\sigma_L = 0.757$ S/m, $\sigma_T = 0.064$ S/m, $R_{res} = 2 \times 10^7$ Ω, $A_n = 25 \times 10^{-6}$ m; $A_w = 10^{-4}$ m; $L_1 = 7.4 \times 10^{-3}$ m; $L_2 = 5 \times 10^{-4}$ m; $L_3 = 5 \times 10^{-4}$ m; and $L_4 = 2.2 \times 10^{-2}$ m.

(preparative) scale electrophoresis apparatus. The method provided an accuracy of approximately 10% of the channel's length (several centimeters in a 29 cm long channel).[14] While this is sufficient for maintaining a stationary ITP interface by counterflow, it is far from the accuracy required in order to deliver a focused sample to a designated order 10−100 μm reaction site. Furthermore, any changes to the conductivities of the buffers (e.g., due to the contents of the sample) modify the relation between location and current, further reducing accuracy.

We here present a novel method for precise and automatic detection of the ITP interface location in a microchannel by current monitoring alone. Our technique uses geometrical constrictions in the microchannel to obtain a unique profile of the current signal during ITP. We first provide an overview of the principle of the method, next present an analytical model for predicting the electric current profile, and finally present experimental results demonstrating the robustness of the method to significant variations in buffer conditions and its ability to deliver the sample to a designated location with a 50 μm accuracy.

■ PRINCIPLE OF THE METHOD

ITP uses a discontinuous buffer system consisting of low mobility (TE) and high mobility (LE) buffers. As ITP propagates, the low conductivity TE displaces the high conductivity LE in the channel, resulting in gradual increase in the overall resistance in the channel and a decrease in current (for an applied constant voltage). When adding geometrical constrictions to the channel (Figure 1a), narrow sections have higher resistance and hence a higher electric field. As a result, the ITP interface travels at a higher velocity in these sections, resulting in what appears as a sharp "step" in the current reading (Figure 1b). Video ac5036345_si_001 of the Supporting Information presents a movie of ITP electro-migration in the channel together with its electric current trace.

While the exact magnitude of the current still depends on buffer conditions, the sharp electric field gradient is associated with a specific spatial location and can be used to accurately detect the location of the interface. We developed an algorithm for detecting these changes in electric current, which is based on a cross-correlation of the electric current signal with a predefined step function (Figure 1c). The algorithm works in real-time and indicates the exact time in which the ITP interface enters the constriction (Figure 1d). The computer can then be set to deliver the sample to a desired location and stop the electric field.

■ THEORY

We here present a simple algebraic model which enables prediction of such electric current curves as a function of the buffers properties and channel geometry.

As illustrated in Figure 2a, we consider a channel consisting of N identical constrictions, each of length L_2, separated by $N - 1$ wide regions of length L_3. The constrictions region is connected to reservoirs on either side through wide sections of lengths L_1 and L_4. Applying constant voltage across the channel, the ITP interface moves along the different regions of the channel. We define $x_p(t)$ as the time-dependent axial position of the ITP interface along the channel, measured from the entrance of the TE reservoir. To obtain an algebraic expression, we choose a discrete approach and indexed each of the wide regions by i, ranging from 1 to $N + 1$.

At any given location of the ITP interface, the total electrical resistance of the channel can be obtained by modeling each section as an individual resistor and summing over all resistors in series. The electric current is then given by

$$I(t) = \frac{V}{R_{r,i}[x_p(t)]} \tag{1}$$

where $R_{r,i}[x_p(t)]$ is the overall resistance of the channel. This resistance is a function of the interface location along the channel, $x_p(t)$, the channel section in which it is located, i, and whether this section is wide or narrow (represented by the index r). We apply an Ohmic model in each region, and assume peak mode ITP, where the characteristic length of the ITP interface is small compared to the characteristic geometrical dimensions. In a wide region i, the total resistance can be expressed as

$$R_{w,i}(x_p(t)) = a_w x_p(t) + b_{w,i}$$

$$a_w = \frac{1}{A_w}\left(\frac{1}{\sigma_T} - \frac{1}{\sigma_L}\right)$$

$$b_{w,i} = \frac{L_2(i-1)}{\sigma_T}\left(\frac{1}{A_n} - \frac{1}{A_w}\right) + \dots$$

$$\dots + \frac{1}{\sigma_L}\left(\frac{L_1 + L_2(i-1) + L_3(N-1) + L_4}{A_w} + \frac{L_2(N+1-i)}{A_n}\right) + R_{res} \tag{2}$$

and in the narrow region i as

$$R_{n,i}(x_p(t)) = a_n x_p(t) + b_{n,i}$$

$$a_n = \frac{1}{A_n}\left(\frac{1}{\sigma_T} - \frac{1}{\sigma_L}\right)$$

$$b_{n,i} = \frac{(L_1 + L_3(i-1))}{\sigma_T}\left(\frac{1}{A_w} - \frac{1}{A_n}\right) + \dots$$

$$\dots + \frac{1}{\sigma_L}\left(\frac{L_3(N-1) + L_4}{A_w} + \frac{L_1 + L_2 \cdot N + L_3(i-1)}{A_n}\right) + R_{res} \tag{3}$$

where the wide and narrow cross-section areas are denoted by A_w and A_n, respectively, and the conductivities of the adjusted TE and LE solutions are denoted by σ_T and σ_L, respectively. R_{res} represents the resistance of both reservoirs (assumed to be constant in time).[15] Thus, the generalized total resistance can be expressed as

$$R_{r,i}[x_p(t)] = a_r x_p(t) + b_{r,i} \tag{4}$$

where a_r and $b_{r,i}$ are the regional index-dependent coefficients.

The ITP velocity, dx_p/dt, is given by the product of the leading ion mobility, μ_L, and the electric field in the LE region, E_L, and can be expressed as

$$\frac{dx_p}{dt} = \mu_L E_L = \frac{\mu_L I(t)}{\sigma_L A_r} \tag{5}$$

where A_r is the cross-section area of region r, occupied by the ITP interface. Substituting eqs 1 and 4 into eq 5 and integrating both sides, we obtain

$$\int_{x_p(t_{r,i})}^{x_p(t)} (a_r x + b_{r,i})\, dx = \int_{t_{r,i}}^{t} \frac{\mu_L V}{\sigma_L A_r}\, d\tau \tag{6}$$

where $t_{r,i}$ is the time in which the interface reaches region r in section i (e.g., $t_{w,2}$), and $x_p(t_{r,i})$ is the location of the interface at the exact same time. The integration yields the quadratic equation

$$a_r[x_p(t)^2 - x_p(t_{r,i})^2] + b_{r,i}[x_p(t) - x_p(t_{r,i})]$$
$$= \frac{\mu_L V}{\sigma_L A_r}(t - t_{r,i}) \tag{7}$$

This equation is readily solved analytically for $x_p(t)$, and its result can be substituted into eq 1 to obtain the electric current trace in time.

■ EXPERIMENTAL SECTION

Channel Design. We designed a 40 mm long microchannel which contains four constrictions, forming three wide chambers (Figure 1a). The width of the wide sections of the channel was set to 100 μm, while the width of the narrow sections in the constriction regions was set to 25 μm. The first constriction was located 10 mm from the entrance to the channel, allowing enough time for ITP to stabilize and for the sample to sufficiently accumulate. Each constriction's length was set to 500 μm, while the wide chambers between constrictions were

250 μm long. Using a mylar mask reflecting this geometry, a 20 μm thick SU8 mold was fabricated at Stanford Microfluidic Foundry (Stanford University, CA, http://www.stanford.edu/group/foundry/) using standard lithography. Using this mold, the microfluidic chips were fabricated in house from PDMS and a cross-linker to monomer ratio of 1:10 via standard protocols.[16]

Experimental Setup. We performed all ITP experiments at a constant voltage of 400 V, using a high voltage source meter (model 2410, Keithley Instruments, Cleveland, OH) controlled by MATLAB (R2011b, Mathworks, Natick, MA). We obtained images using an inverted epifluorescent microscope (Ti−U, Nikon, Tokyo, Japan) equipped with a metal halide light source (Intensilight, Nikon Japan), a 4X (NA = 0.13, WD = 17.2 mm) Nikon PlanApo objective, and a Chroma 49006 filter-cube (620/60 nm excitation, 700/75 nm emission, and 660 nm dichroic mirror). Images were captured using a 16 bit, 2560 × 2160 pixel array CMOS camera (Neo, Andor, Belfast Ireland) cooled to −40 °C and processed with MATLAB. The camera was controlled by NIS Elements (v.4.13, Nikon, Tokyo, Japan). We measured buffer conductivities in the reservoirs using a conductivity meter (PC700, Eutech Instruments, The Netherlands).

Isotachophoresis Assay. We performed the ITP experiments using LE buffer composed of 100 mM HCl, 200 mM bistris, and 1% 1.3 MDa poly(vinylpyrrolidone) (PVP) for suppression of electroosmotic flow (EOF).[17] For the contamination experiments (Figure 4), we spiked the LE with NaOH at concentrations of 10, 20, 40, and 50 mM. We used Dylight 650 (Thermo Fisher Scientific, Waltham, MA) as our sample, due to its known photostability. Tricine, bistris, and PVP were obtained from Sigma-Aldrich (St. Louis, MO). HCl was obtained from Merck (Darmstadt, Germany), and NaOH from Bio-Lab Ltd. (Jerusalem, Israel). All buffer stock solutions were prepared in 20 mL glass bottles and kept at room temperature. All buffer solutions were prepared using deionized water (DI) from Sigma-Aldrich (St. Louis, MO).

We filled the LE reservoir with 20 μL of LE solution and filled the channel by applying vacuum from the other reservoir for 2 min. We then rinsed the TE reservoir with DI and filled it with 18 μL of TE solution and 2 μL of 10 nM Dylight. We turned on the electric field and set the algorithm to turn off the electric field when the ITP plug reaches the second chamber.

Location Detection Algorithm. As shown in Figure 1 and discussed in the theory section, as the ITP plug enters the constrictions, a rapid and sharp decrease in the current occurs, resulting as a step pattern in the current signal. Our algorithm is designed to detect these steps in real-time, indicating the exact time of entrance into the constriction. In each experiment, the electric current is normalized by its initial value (Figure 4a). This guarantees that a single set of parameters could be used regardless of the specific conductivities of the buffers. The normalized signal is smoothed in real-time using a seven neighbors median filter. The change of slope in the electric current could, in principle, be detected by numerically computing the local gradient. However, this method is very sensitive to noise. Instead, as illustrated in Figure 1c, we define a backward facing step function whose magnitude is 0.5 and spans over 11 points. At each point in time, this step function is centered on the electric current value and the two functions are cross-correlated with one another. As shown in Figure 1d, the resulting correlation signal is characterized by distinct peaks, whose maxima corresponds to the point in time in which the

interface enters the constriction (red circles in Figure 1, panels b and d). As can be seen in Figure 1d, the peaks have a high signal-to-noise ratio, and based on several experiments, we determined a threshold value (set to 0.04) that distinguishes between the true peaks and the noise. The location of the interface can then be determined based on the number of peaks counted, and the ITP interface can be stopped at the desired chamber. While the algorithm detects the time at which the ITP plug enters into the constriction, a short preprogramed time delay can be used to stop the plug in the following wide chamber. In doing so, one must account for an inherent time delay when the control program is implemented in software. Video ac5036345_si_002 of the Supporting Information presents a dynamic illustration of the correlation process.

■ RESULTS AND DISCUSSION

Model Validation. Figure 2b represents the model results showing a time trace of the electric current for a geometry consisting of four constrictions. Figure 2c presents a comparison between our model prediction and the experimental results. We analytically solved eq 7 for $x_p(t)$, using MATLAB, and substitute it into eq 1 to obtain the electric current at any point in time. We obtained all model parameters (lengths of the sections, conductivities of the buffers) from direct measurements and used PeakMaster[18] and Spresso[19] to calculate the adjusted TE conductivity. The only free-parameter in the system is the resistance of the reservoirs, R_{res}. We choose its value ($R_{res} = 2 \times 10^7$ Ω) such that the first step in the model and in the experimental results coincide in time. This value is consistent with estimates provided by Persat et al. for the resistance of the reservoir.[20] Results show that the model accurately predicts both the magnitude and duration of the electric current steps.

Sample Delivery Accuracy. Figure 3a presents a sequence of raw fluorescence images of ITP electromigration, using 1 nM of Dylight to indicate the location of the interface. As the ITP interface enters a constriction, the automatic tracking algorithm detects the ITP plug location and turns off the electric field as it enters the second chamber of the channel (after the second constriction). Figure 3b shows the resulting stop locations of five repeats of the experiment. We define the stop location as the location of the maxima of the width-averaged intensity signal. The red dashed lines represent the range of 95% confidence on the mean location, assuming a student's t-distribution. Results show that the algorithm is able to stop the ITP plug with an accuracy of 50 μm. Video ac5036345_si_003 of the Supporting Information presents a movie in which a focused sample is delivered to a designated chamber.

Robustness to Contamination. In many practical applications (e.g., in urine or blood analysis), samples may have a significant ion concentration which affects the conductivity, pH, or both. This in turn may affect the ITP velocity and the electric current trace. Figure 4a presents the electric current versus time, for the same LE buffer spiked with 10, 20, 40, and 50 mM NaOH (final concentrations in the reservoir). As expected, the additional sodium concentration results in overall higher electric current values as well as a higher ITP velocity. For this reason, standard current monitoring is not sufficiently accurate (i.e., the same current value corresponds to drastically different locations at different conductivities). As our method is based on detecting changes in the slope of the current, it is far less sensitive to buffer conditions. Figure 4b presents the stopping locations obtained
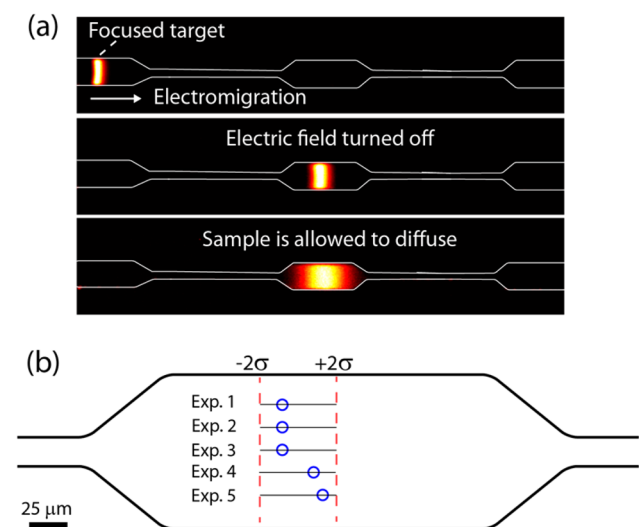
Figure 3. (a) Raw fluorescence images showing the delivery of an ITP plug to a desired location. Upon arrival to the second chamber, the electric field is turned off and the sample is allowed to diffuse. (b) Experimental results demonstrating the accuracy of the technique. Blue ○ represent the stop locations of five experiments, in which the algorithm was set to turn off the electric field after the ITP plug exits the second constriction. We define the stopping point as the location of the maximal signal of the width-averaged intensity. Red dashed lines represent the range of 95% confidence on the mean location and show a 50 μm accuracy in sample delivery.
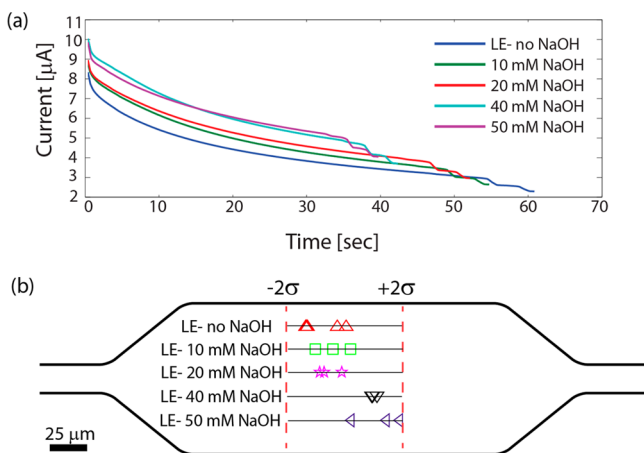

Figure 4. Experimental results demonstrating the robustness of the methods to significant contamination of the LE. (a) Electric current vs time for ITP performed using LE spiked with NaOH concentrations between 0 and 50 mM. As expected, the absolute values of the current as well as its rate of change vary significantly between experiments. The electric current value thus cannot be used to robustly detect the location of the ITP interface. (b) Experimental results showing the automatically obtained stop locations, with the LE spiked with NaOH concentration between 0 and 50 mM (five repeats of pure LE case and three repeats for all other cases). Red dashed lines represent a 95% confidence on the mean, accounting for all cases and repeats. Results show the algorithm is insensitive to such contaminations and can deliver the focused sample to a desired location with an accuracy of 70 μm.

for different sodium concentrations in the LE (three repeats for each condition, and five repeats for the pure system). All cases were run using the exact same algorithm parameters. Red dashed lines represent a 95% confidence on the mean,

accounting for all cases and repeats. Results show that the algorithm worked well for all cases and is robust to significant contaminations of the LE, with a total accuracy of 70 μm.

■ CONCLUSIONS

We demonstrated the use of the technique to deliver sample to a designated location in the channel with an accuracy of 50 μm (pure LE) or 70 μm (LE "contaminated" with as much as 50 mM of NaOH). The direct use of this technique is in allowing longer reaction times between focused samples and immobilized surface probes in ITP-based surface reactions.[9] Clearly, the delivery accuracy could be further optimized based on the specific requirement and constraints of each implementation. The analytical model we provided could be used to predict the electric current curves for arbitrary constriction geometries and applied voltages and thus assist in such optimizations. For example, having smaller constrictions would result in sharper features in the electric current curve, which would be easier to detect. However, this would also result in faster transition of the interface through the constriction, which make precise stopping of the voltage more challenging. Furthermore, a major source of inaccuracy in our current implementation is likely due to the use of a MATLAB code as the controller (for both sampling the current and commanding the voltage stop). Implementation of the controller in hardware would allow higher accuracy and faster response times.

The technique may also be useful for other purposes such as control of light shutters before passing through a detection location (e.g., to avoid photobleaching) or switching of the electric field from one reservoir to another (e.g., to initiate transient ITP). In general, it could be used for sequencing a chain of events occurring as the ITP interface passes through the channel. We believe that the relatively high accuracy of the method, together with its simplicity would make it a useful tool in ITP-based diagnostic assays.

■ ASSOCIATED CONTENT

Ⓢ Supporting Information

Video showing the electric current trace as the ITP interface electromigrates through multiple constrictions (ac5036345_si_001). Video illustrating the operation of the cross-correlation algorithm for detecting the location of the ITP interface (ac5036345_si_002). Video demonstrating the delivery of a focused sample to a desired site (ac5036345_si_003). This material is available free of charge via the Internet at http://pubs.acs.org.

■ AUTHOR INFORMATION

Corresponding Author
*E-mail: mberco@technion.ac.il.

Notes

The authors declare no competing financial interest.

■ ACKNOWLEDGMENTS

■ REFERENCES

(1) Everaerts, F. M.; Beckers, J. L.; Verheggen, T. P. E. M. *Isotachophoresis: Theory, Instrumentation and Applications*; Elsevier: Amsterdam; 2011.

(2) Gebauer, P.; Malá, Z.; Boček, P. *Electrophoresis* **2007**, *28*, 26−32.

(3) Bercovici, M.; Han, C. M.; Liao, J. C.; Santiago, J. G. *Proc. Natl. Acad. Sci. U.S.A.* **2012**, *109*, 11127−11132.

(4) Persat, A.; Santiago, J. G. *Anal. Chem.* **2011**, *83*, 2310−2316.

(5) Bercovici, M.; Kaigala, G. V.; Mach, K. E.; Han, C. M.; Liao, J. C.; Santiago, J. G. *Anal. Chem.* **2011**, *83*, 4110−4117.

(6) Eid, C.; Garcia-Schwarz, G.; Santiago, J. G. *Analyst* **2013**, *138*, 3117−3120.

(7) Garcia-Schwarz, G.; Santiago, J. G. *Anal. Chem.* **2012**, *84*, 6366−6369.

(8) Garcia-Schwarz, G.; Santiago, J. G. *Angew. Chem.* **2013**, *125*, 11748−11751.

(9) Karsenty, M.; Rubin, S.; Bercovici, M. *Anal. Chem.* **2014**, *86*, 3028−3036.

(10) Han, C. M.; Katilius, E.; Santiago, J. G. *Lab Chip* **2014**, *14*, 2958.

(11) Khnouf, R.; Goet, G.; Baier, T.; Hardt, S. *Analyst* **2014**, *139*, 4564−4571.

(12) Huang, X.; Gordon, M. J.; Zare, R. N. *Anal. Chem.* **1988**, *60*, 1837−1838.

(13) Reinhoud, N. J.; Tjaden, U. R.; van der Greef, J. *J. Chromatogr. A* **1994**, *673*, 239−253.

(14) Harrison, S. L. M.; Ivory, C. F. *J. Sep. Sci.* **2007**, *30*, 3255−3261.

(15) Persat, A.; Chambers, R. D.; Santiago, J. G. *Lab Chip* **2009**, *9*, 2437−2453.

(16) Duffy, D. C.; McDonald, J. C.; Schueller, O. J. A.; Whitesides, G. M. *Anal. Chem.* **1998**, *70*, 4974−4984.

(17) Milanova, D.; Chambers, R. D.; Bahga, S. S.; Santiago, J. G. *Electrophoresis* **2012**, *33*, 3259−3262.

(18) Hruška, V.; Jaroš, M.; Gaš, B. *Electrophoresis* **2006**, *27*, 984−991.

(19) Bercovici, M.; Lele, S. K.; Santiago, J. G. *J. Chromatogr. A* **2009**, *1216*, 1008−1018.

(20) Persat, A.; Suss, M. E.; Santiago, J. G. *Lab Chip* **2009**, *9*, 2454−2469.